

# Journal of Materials Chemistry C

Accepted Manuscript



This is an *Accepted Manuscript*, which has been through the Royal Society of Chemistry peer review process and has been accepted for publication.

*Accepted Manuscripts* are published online shortly after acceptance, before technical editing, formatting and proof reading. Using this free service, authors can make their results available to the community, in citable form, before we publish the edited article. We will replace this *Accepted Manuscript* with the edited and formatted *Advance Article* as soon as it is available.

You can find more information about *Accepted Manuscripts* in the [Information for Authors](#).

Please note that technical editing may introduce minor changes to the text and/or graphics, which may alter content. The journal's standard [Terms & Conditions](#) and the [Ethical guidelines](#) still apply. In no event shall the Royal Society of Chemistry be held responsible for any errors or omissions in this *Accepted Manuscript* or any consequences arising from the use of any information it contains.

Cite this: DOI: 10.1039/coxx00000x

www.rsc.org/xxxxxx

ARTICLE TYPE

# Controlling and revealing trap distributions of $\text{Ca}_6\text{BaP}_4\text{O}_{17}:\text{Eu}^{2+},\text{R}^{3+}$ (R=Dy, Tb, Ce, Gd, Nd) by codoping different trivalent lanthanides

Haijie Guo, Yuhua Wang\*, Wenbo Chen, Wei Zeng, Shaochun Han, Gen Li, Yanyan Li

Received (in XXX, XXX) Xth XXXXXXXXX 20XX, Accepted Xth XXXXXXXXX 20XX

DOI: 10.1039/b000000x

Thermoluminescence (TL) glow curves of  $\text{Ca}_6\text{BaP}_4\text{O}_{17}:\text{Eu}^{2+},\text{R}^{3+}$  (R=Dy, Tb, Ce, Gd, Nd) samples were measured above room temperature in order to compare the trap distributions in the band gap. The observed phenomenon indicates that  $\text{R}^{3+}$  ions (R=Dy, Tb, Ce, Gd, Nd) have different effects on trap properties of  $\text{Ca}_6\text{BaP}_4\text{O}_{17}:\text{Eu}^{2+}$  phosphor. The most shallow trap (0.620 eV) for  $\text{Tb}^{3+}$  ion and the deepest trap (0.762 eV) for  $\text{Dy}^{3+}$  ion eventually led to shorter duration (4.3 h and 1.2 h respectively), while appropriate trap depth (0.716 eV) for  $\text{Nd}^{3+}$  ion makes  $\text{Ca}_6\text{BaP}_4\text{O}_{17}:\text{Eu}^{2+},\text{Nd}^{3+}$  sample show the longest afterglow duration (37.9 h). Codoping with  $\text{Tb}^{3+}$  ion slightly increases the instinct traps of  $\text{Ca}_6\text{BaP}_4\text{O}_{17}:\text{Eu}^{2+}$  sample and creates a new low-temperature TL peak corresponding to relatively shallow trap leading to the strongest initial afterglow brightness (0.887  $\text{cd/m}^2$ ), while, codoping with other  $\text{R}^{3+}$  ions (R=Dy, Ce, Gd, Nd) creates new appropriate or inappropriate traps. By performing a series of long-lasting phosphorescence (LLP) spectra with various irradiated time and TL experiments with varying delay time after ceasing the UV irradiation, the trap distribution of the depth and shape was evaluated. The result provides a better understanding of the role of these trapping centers played in the persistent luminescent mechanism.

## 1. Introduction

Long-lasting phosphorescence (LLP) materials emitting light several hours after ceasing the irradiation source, a special case of thermally stimulated luminescence, results from a gradual release of charge carriers from trapping centers induced by the thermal disturbance at room temperature.<sup>1</sup> The deeper the depth of the traps, the higher energy needed to release these charge carriers. Knowledge of these trap depths is thus of crucial importance in the understanding of the LLP mechanism. Besides, LLP materials can be widely applied in various fields such as optical storage media<sup>2</sup> as well as sensors for structural damage, fracture of materials,<sup>3-5</sup> and vivo-imaging<sup>6</sup>. These applications also demand the exact knowledge of the LLP mechanism and the trap identification.

Divalent europium and trivalent lanthanides codoped phosphors acting as long persistence materials have been researched in-depth and extensively applied in business. It is generally believed that  $\text{Eu}^{2+}$  ion acts as the activator, while other trivalent lanthanides produce new traps due to nonequivalent substitution<sup>7</sup> or at least modify the intrinsic trap properties in these phosphors. Actually, the previous knowledge of  $\text{Eu}^{2+}$  ion activated persistent phosphors is mainly based on aluminates and silicates, e.g.  $\text{Sr}_2\text{MgSi}_2\text{O}_7:\text{Eu}^{2+},\text{Dy}^{3+}$  (blue),<sup>8</sup>  $\text{Sr}_4\text{Al}_4\text{O}_{25}:\text{Eu}^{2+},\text{Dy}^{3+}$  (blue),<sup>9</sup>  $\text{SrAl}_2\text{O}_4:\text{Eu}^{2+},\text{Dy}^{3+}$  (green),<sup>10</sup> all of which can continue emitting light more than 24 h in the dark. However, detailed research on phosphates as host for persistent phosphors is very few so far.

Recently, Cheetham and co-workers first discovered the host  $\text{Ca}_6\text{BaP}_4\text{O}_{17}$  and reported that  $\text{Ca}_6\text{BaP}_4\text{O}_{17}:\text{Eu}^{2+}$  can emit a strong yellow light peaked at 553 nm under excitation with UV to blue light and has a higher color-rendering index than that of  $\text{YAG}:\text{Ce}^{3+}$ .<sup>11</sup> Besides, in previous paper, we reported the persistent luminescence in  $\text{Ca}_6\text{BaP}_4\text{O}_{17}:\text{Eu}^{2+},\text{Ho}^{3+}$  and found that the incorporation of the  $\text{Ho}^{3+}$  ion into the  $\text{Ca}_6\text{BaP}_4\text{O}_{17}:\text{Eu}^{2+}$  phosphor can greatly enhance its persistent luminescence behavior.<sup>12</sup> Based on the above discussion, we predict that  $\text{Ca}_6\text{BaP}_4\text{O}_{17}:\text{Eu}^{2+}$  may have the potential to serve as an attractive candidate for yellow LLP phosphor and thus enrich the long-wavelength LLP phosphors urgent needed in particular fields such as solar energy utilization<sup>13</sup> and in vivo bioimaging.<sup>6</sup> Measurement of the thermoluminescence (TL) glow curves is a versatile tool to determine the number as well as the depth of the traps in materials.<sup>14</sup> The too shallow trap depth will result in a relatively short afterglow, while, if the trap is too deep, no charge carriers can escape because thermal energy is not enough and no persistent luminescence will be observed at room temperature.<sup>15</sup> In the present work, the TL measurements of  $\text{Ca}_6\text{BaP}_4\text{O}_{17}:\text{Eu}^{2+},\text{R}^{3+}$  (R=Dy, Tb, Ce, Gd, Nd) were carried out between 25 and 400 °C. The trap depths and densities in these materials were derived from the TL glow curves. The traps distribution was estimated by performing a series of LLP spectra with various irradiated time and TL experiments with varying delay time after ceasing the UV irradiation, and thus the effect of the  $\text{R}^{3+}$  ions codoping on the LLP luminescence and TL of  $\text{Ca}_6\text{BaP}_4\text{O}_{17}:\text{Eu}^{2+},\text{R}^{3+}$  (R=Dy, Tb, Ce, Gd, Nd) phosphors were

discussed according to the results obtained.

## 2. Experimental

A series of samples of  $\text{Ca}_6\text{BaP}_4\text{O}_{17}:0.02\text{Eu}^{2+}$  and  $\text{Ca}_6\text{BaP}_4\text{O}_{17}:0.02\text{Eu}^{2+},0.015\text{R}^{3+}$  (R=Dy, Tb, Ce, Gd, Nd) were synthesized by high-temperature solid-state reaction technique. The starting materials were  $\text{CaCO}_3$  (A.R.),  $\text{BaCO}_3$  (99.99%),  $\text{NH}_4\text{H}_2\text{PO}_4$  (A.R.),  $\text{Eu}_2\text{O}_3$  (99.99%) and other rare earth oxides ( $\text{Dy}_2\text{O}_3$ ,  $\text{Tb}_4\text{O}_7$ ,  $\text{CeO}_2$ ,  $\text{Gd}_2\text{O}_3$ ,  $\text{Nd}_2\text{O}_3$ , typically 99.9%). The stoichiometric mixture of starting materials was ground for 30 min in an agate mortar to form homogeneous fine power mixture by adding an appropriate amount of ethanol. Subsequently, the mixture were fired at 1280 °C for 10 h under a flowing  $\text{N}_2\text{-H}_2$  (95:5) reductive atmosphere in a tube furnace and the relative heating rate is 5 °C/min. After annealing, the samples were cooled to room temperature in the furnace and ground again to powder for subsequent use.

The phases of samples were identified by a Rigaku D/Max-2400 X-ray diffractometer (XRD) using a Rigaku diffractometer with Nifiltered Cu K $\alpha$  radiation at scanning steps of 0.02° in the 2 $\theta$  range from 10° to 80°. The LLP spectra were measured by a FLS-920T fluorescence spectrophotometer with 365 nm as the excitation source. Afterglow decay curve measurements were measured with a PR305 long afterglow instrument after the samples were irradiated with UV light for 10 min. The TL curves were measured with a FJ-427A TL meter (Beijing Nuclear Instrument Factory) with a heating rate of 1 K s<sup>-1</sup> in the temperature range from 20 to 400 °C. Before measurement, 0.0001 g samples pressed in pellets were exposed to the UV light for 2 min.

## 3. Results and discussion

### 3.1. Phase identification.

Fig. 1 shows the XRD patterns of  $\text{Ca}_6\text{BaP}_4\text{O}_{17}:0.02\text{Eu}^{2+}$  and  $\text{Ca}_6\text{BaP}_4\text{O}_{17}:0.02\text{Eu}^{2+},0.015\text{R}^{3+}$  (R=Dy, Tb, Ce, Gd, Nd) compounds. All the XRD patterns have similar diffraction patterns and are in good agreement with previous reports.<sup>12</sup> No impurity peak is detected in the compounds, indicating that the doping ions of  $\text{Eu}^{2+}/\text{R}^{3+}$  are incorporated into the host lattice successfully and hardly change the lattice structure. The rare earth ions are supposed to replace calcium ions due to the consideration of ionic radii matching.<sup>11</sup>

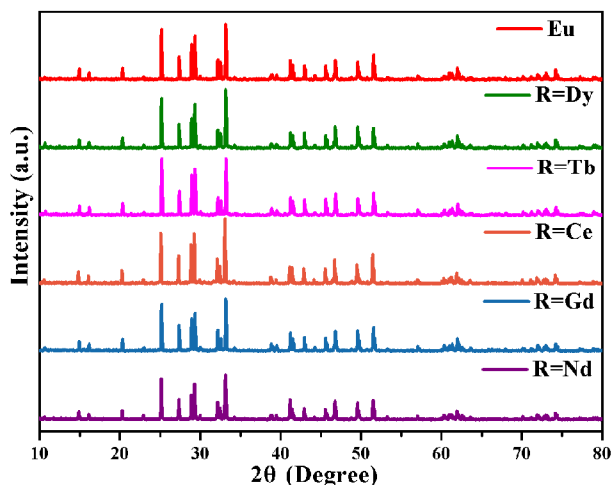


Fig. 1 XRD patterns of  $\text{Ca}_6\text{BaP}_4\text{O}_{17}:\text{Eu}^{2+}$  and  $\text{Ca}_6\text{BaP}_4\text{O}_{17}:\text{Eu}^{2+},\text{R}^{3+}$  (R=Dy, Tb, Ce, Gd, Nd).

### 3.2. Phosphorescence properties of $\text{Ca}_6\text{BaP}_4\text{O}_{17}:\text{Eu}^{2+}$ and $\text{Ca}_6\text{BaP}_4\text{O}_{17}:\text{Eu}^{2+},\text{R}^{3+}$ (R=Dy, Tb, Ce, Gd, Nd).

After removal of the UV excitation at room temperature, yellow LLP is observed in  $\text{Ca}_6\text{BaP}_4\text{O}_{17}:\text{Eu}^{2+}$  and  $\text{Ca}_6\text{BaP}_4\text{O}_{17}:\text{Eu}^{2+},\text{R}^{3+}$ . As shown in Fig. 2, The initial LLP emission profiles and peaks of  $\text{Ca}_6\text{BaP}_4\text{O}_{17}:\text{Eu}^{2+},\text{R}^{3+}$  are similar to that of  $\text{Ca}_6\text{BaP}_4\text{O}_{17}:\text{Eu}^{2+}$  and only the characteristic broad band emission of  $\text{Eu}^{2+}$  ion with the maximum at about 553 nm is observed corresponding to the 5d-4f transition. We can see from Fig. 2 that  $\text{Ca}_6\text{BaP}_4\text{O}_{17}:\text{Eu}^{2+}$ ,  $\text{Ca}_6\text{BaP}_4\text{O}_{17}:\text{Eu}^{2+},\text{Tb}^{3+}$  and  $\text{Ca}_6\text{BaP}_4\text{O}_{17}:\text{Eu}^{2+},\text{Ce}^{3+}$  samples exhibit relatively stronger initial LLP intensity and it gradually increases with prolonged irradiated time. It could be speculated that there are some shallow traps and the trapped carriers need relatively low activation energy to escape from traps at room temperature. On the contrary, in other two samples (codoped with  $\text{Nd}^{3+}$  or  $\text{Gd}^{3+}$  ions), the yellow initial LLP intensity is below 10 times more. It could be making sense that there are some traps with deep depth and the captured charge carriers by the traps are relatively difficult to be released at room temperature which weakened the initial LLP intensity but prolong duration time due to the traps depth is not too deep.<sup>16</sup> Only for the sample codoped with  $\text{Dy}^{3+}$  ion, the initial LLP brightness is the lowest, and its intensity almost has no change with the increase of the irradiated time. We deem that no effective trap exists or the traps depth is too deep resulting that only a small amount of captured charge carriers can be released at room temperature.

70

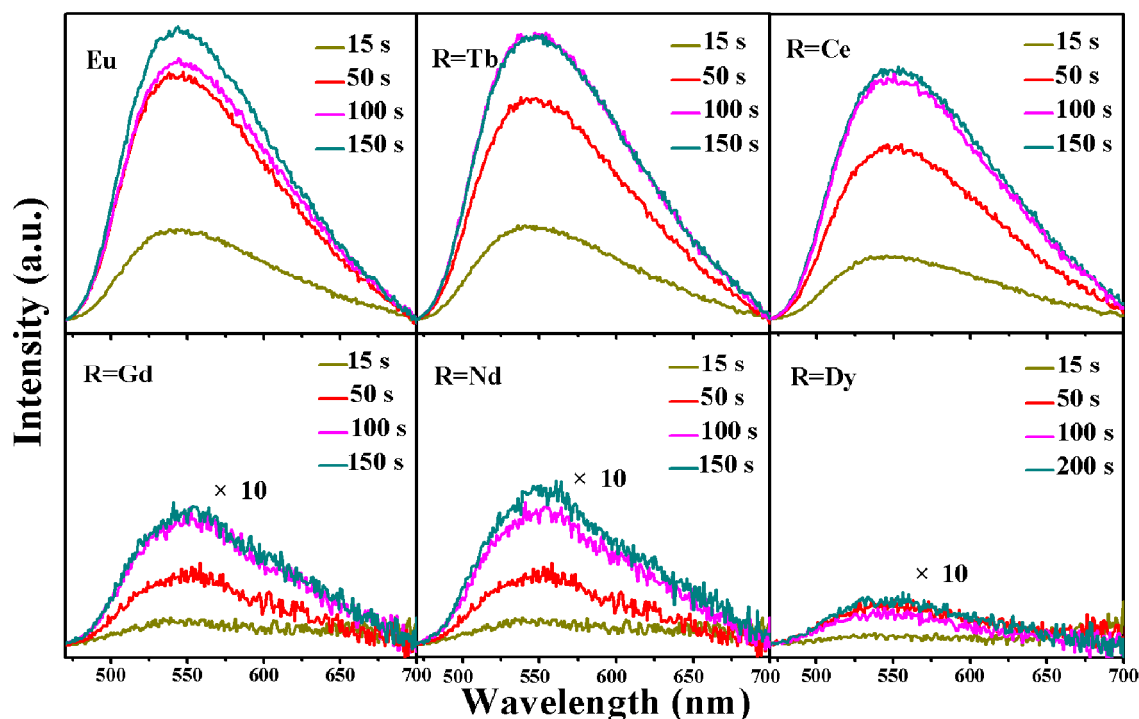


Fig. 2 LLP spectra of  $\text{Ca}_6\text{BaP}_4\text{O}_{17}:\text{Eu}^{2+}$  and  $\text{Ca}_6\text{BaP}_4\text{O}_{17}:\text{Eu}^{2+},\text{R}^{3+}$  ( $\text{R}=\text{Dy}, \text{Tb}, \text{Ce}, \text{Gd}, \text{Nd}$ ) measured with varying the UV irradiation duration.

### 3.3. Afterglow decay curves of $\text{Ca}_6\text{BaP}_4\text{O}_{17}:\text{Eu}^{2+}$ and $\text{Ca}_6\text{BaP}_4\text{O}_{17}:\text{Eu}^{2+},\text{R}^{3+}$ ( $\text{R}=\text{Dy}, \text{Tb}, \text{Ce}, \text{Gd}, \text{Nd}$ ).

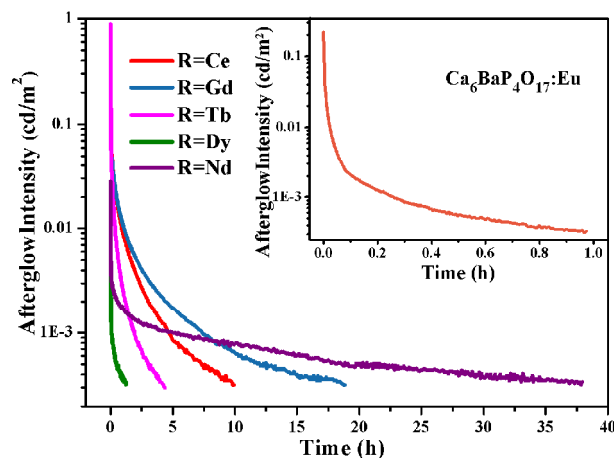


Fig. 3 Afterglow decay curves of  $\text{Ca}_6\text{BaP}_4\text{O}_{17}:\text{Eu}^{2+},\text{R}^{3+}$  ( $\text{R}=\text{Dy}, \text{Tb}, \text{Ce}, \text{Gd}, \text{Nd}$ ); (inset) The afterglow decay curve of  $\text{Ca}_6\text{BaP}_4\text{O}_{17}:\text{Eu}^{2+}$ .

The yellow persistent performance of  $\text{Ca}_6\text{BaP}_4\text{O}_{17}:\text{Eu}^{2+}$  and  $\text{Ca}_6\text{BaP}_4\text{O}_{17}:\text{Eu}^{2+},\text{R}^{3+}$  ( $\text{R}=\text{Dy}, \text{Tb}, \text{Ce}, \text{Gd}, \text{Nd}$ ) was systematically investigated. Fig. 3 depicts the afterglow decay curves of  $\text{Ca}_6\text{BaP}_4\text{O}_{17}:\text{Eu}^{2+}$  and  $\text{Ca}_6\text{BaP}_4\text{O}_{17}:\text{Eu}^{2+},\text{R}^{3+}$  ( $\text{R}=\text{Dy}, \text{Tb}, \text{Ce}, \text{Gd}, \text{Nd}$ ) which excited by UV light for 10 min. All the detailed results about the initial afterglow brightness and the afterglow duration of  $\text{Ca}_6\text{BaP}_4\text{O}_{17}:\text{Eu}^{2+}$  and  $\text{Ca}_6\text{BaP}_4\text{O}_{17}:\text{Eu}^{2+},\text{R}^{3+}$  ( $\text{R}=\text{Dy}, \text{Tb}, \text{Ce}, \text{Gd}, \text{Nd}$ ) are presented in Table 1. The sample  $\text{Ca}_6\text{BaP}_4\text{O}_{17}:\text{Eu}^{2+},\text{Tb}^{3+}$  has the optimum initial brightness reaching about  $0.887 \text{ cd/m}^2$  and  $\text{Ca}_6\text{BaP}_4\text{O}_{17}:\text{Eu}^{2+},\text{Nd}^{3+}$  sample has the longest lasting time lasting near 37.9 h above the recognizable intensity level ( $0.32 \text{ mcd/m}^2$ ) than the other samples. We thus conclude that the different  $\text{R}^{3+}$  ( $\text{R}=\text{Dy}, \text{Tb}, \text{Ce}, \text{Gd}, \text{Nd}$ )

ions codoping has a great influence on the afterglow performance.

**Table 1** Initial afterglow brightness and afterglow duration of  $\text{Ca}_6\text{BaP}_4\text{O}_{17}:\text{Eu}^{2+}$  and  $\text{Ca}_6\text{BaP}_4\text{O}_{17}:\text{Eu}^{2+},\text{R}^{3+}$  ( $\text{R}=\text{Dy}, \text{Tb}, \text{Ce}, \text{Gd}, \text{Nd}$ ).

R	Eu	Dy	Tb	Ce	Gd	Nd
Initial afterglow brightness ( $\text{cd/m}^2$ )	0.221	0.021	0.887	0.400	0.206	0.028
Afterglow duration (h)	0.975	1.233	4.333	9.917	18.83 3	37.91 7

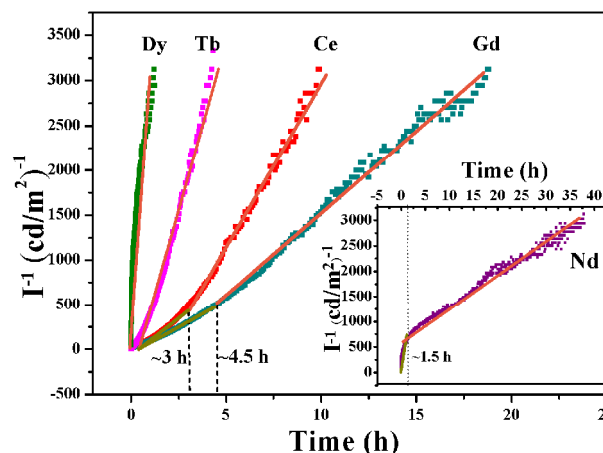


Fig. 4 Function of reciprocal afterglow intensity ( $I^{-1}$ ) versus time ( $t$ ) of  $\text{Ca}_6\text{BaP}_4\text{O}_{17}:\text{Eu}^{2+},\text{R}^{3+}$  ( $\text{R}=\text{Dy}, \text{Tb}, \text{Ce}, \text{Gd}, \text{Nd}$ ) excited for 10 min.

The afterglow decay curves of  $\text{Ca}_6\text{BaP}_4\text{O}_{17}:\text{Eu}^{2+},\text{R}^{3+}$  ( $\text{R}=\text{Dy}, \text{Tb}, \text{Ce}, \text{Gd}, \text{Nd}$ ) were also plotted as a function of reciprocal persistent luminescence intensity ( $I^{-1}$ ) versus time ( $t$ ), as shown in

Fig. 4. For the samples codoped with  $\text{Dy}^{3+}$  or  $\text{Tb}^{3+}$  ions, the  $I^l-t$  curves at all the delay period can be fitted by a straight line approximately. The linear dependence of  $I^l$  versus  $t$  indicates that the LLP luminescence in  $\text{Ca}_6\text{BaP}_4\text{O}_{17}:\text{Eu}^{2+},\text{R}^{3+}$  ( $\text{R}=\text{Dy}, \text{Tb}$ ) phosphors is mainly caused by an effective trap center. However, all the  $I^l-t$  curves of  $\text{Ca}_6\text{BaP}_4\text{O}_{17}:\text{Eu}^{2+},\text{R}^{3+}$  ( $\text{R}=\text{Nd}, \text{Ce}, \text{Gd}$ ) could be divided into two parts. The latter linear dependence of  $I^l$  versus  $t$  indicates that long-lasting persistent luminescence in  $\text{Ca}_6\text{BaP}_4\text{O}_{17}:\text{Eu}^{2+},\text{R}^{3+}$  ( $\text{R}=\text{Nd}, \text{Ce}, \text{Gd}$ ) phosphors probably occurs through a tunneling-related process.<sup>17,18</sup> The tunneling effect is slow and always occurs alongside the retrapping effect in the late stage of decay.<sup>19</sup> Due to the retrapping effect, the recombination rate of charge carriers would be slower, leading to relatively weaker LLP intensity but longer LLP duration time during the slow-decay process, which will be discussed later according to the results of TL spectra.

### 3.4. TL and fading experiments of $\text{Ca}_6\text{BaP}_4\text{O}_{17}:\text{Eu}^{2+}$ and $\text{Ca}_6\text{BaP}_4\text{O}_{17}:\text{Eu}^{2+},\text{R}^{3+}$ ( $\text{R}=\text{Dy}, \text{Tb}, \text{Ce}, \text{Gd}, \text{Nd}$ ).

Fig. 5 presents the TL spectra of  $\text{Ca}_6\text{BaP}_4\text{O}_{17}:\text{Eu}^{2+},\text{R}^{3+}$  ( $\text{R}=\text{Dy}, \text{Tb}, \text{Ce}, \text{Gd}, \text{Nd}$ ) and the results show that the intensity of the TL glow curves and the maximum temperature of the TL peaks of  $\text{Ca}_6\text{BaP}_4\text{O}_{17}:\text{Eu}^{2+},\text{R}^{3+}$  are differ from each other. The intensity of the TL glow curve is related to the amount of trapped charge carriers, and the maximum temperature of the TL peak provides information on the depth of the charge carriers trap. Apparently, the trap depth can be tuned by changing the species of the codopant owing to the various electron affinity and ionization energy of trivalent lanthanides.<sup>13,20</sup> The shallow traps have contribution for the initial intensity of the afterglow, and the deep traps make contribution for the duration.<sup>21,22</sup> The effective TL peak is situated slightly above room temperature (320-400 K), which is a temperature leading to better LLP properties.<sup>23,24</sup> The trap depths can be calculated by the Urbach method<sup>13, 25</sup>

$$E = \frac{T_m}{500} \quad (1)$$

where  $T_m$  is the peak temperature (in Kelvin). The estimated trap depths for the glow peak are showed in Fig. 6. The corresponding TL glow peak maxima predict that codoping  $\text{Tb}^{3+}$  ion provides the most shallow trap (0.620 eV) while  $\text{Dy}^{3+}$  ion yields the deepest trap (0.762 eV). There is thus a clear correlation between the TL and initial LLP intensity, in which the higher intensity and the lower the maximum temperature of the TL peak, the stronger the initial LLP emission intensity and *vice versa*. It thus appears that the trap depth (0.716 eV) is optimal for an optimized LLP luminescence and  $\text{Nd}^{3+}$  ion acts as the best electron trap in  $\text{Ca}_6\text{BaP}_4\text{O}_{17}:\text{Eu}^{2+}$ .

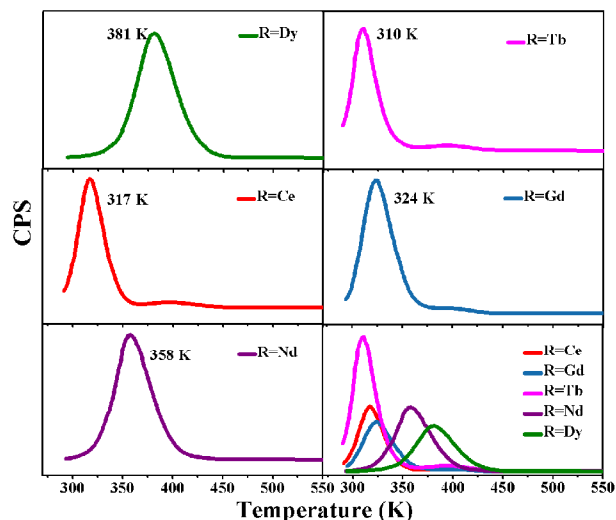


Fig. 5 The TL spectra of  $\text{Ca}_6\text{BaP}_4\text{O}_{17}:\text{Eu}^{2+},\text{R}^{3+}$  ( $\text{R}=\text{Dy}, \text{Tb}, \text{Ce}, \text{Gd}, \text{Nd}$ ).

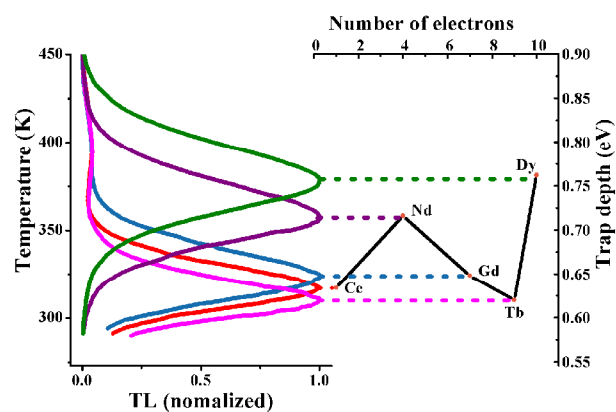


Fig. 6 The trap depth of experimental measured from TL glow peak maxima.

In order to further investigate the trap structure in different codopants phosphors, the fading of TL was measured with different delay time after ceasing the UV irradiation.<sup>26,27</sup> For the samples codoped with  $\text{Dy}^{3+}/\text{Tb}^{3+}$  ions as shown in Fig. 7, there only exists one or three discrete trap depth distribution due to the reason that the location of the peak maximum is independent of the duration. Codoping with  $\text{Tb}^{3+}$  ion creates a new low-temperature TL peak corresponding to the relatively shallow trap and slightly enhances the instinct traps of  $\text{Ca}_6\text{BaP}_4\text{O}_{17}:\text{Eu}^{2+}$ , which may be caused by calcium vacancy ( $\text{V}_{\text{Ca}}$ ) and oxygen vacancy ( $\text{V}_{\text{O}}$ ). From the viewpoint of conservation of charge, the substitution of  $\text{Tb}^{3+}$  for  $\text{Ca}^{2+}$  would impede the occurrence of oxygen vacancies and more calcium vacancies are needed to maintain the charge balance. However, the coordination center of oxygen ions will disappear due to the occurrence of the calcium vacancies, hence the concentration of oxygen vacancy is also enhanced in  $\text{Ca}_6\text{BaP}_4\text{O}_{17}:\text{Eu}^{2+},\text{Tb}^{3+}$  sample.<sup>28</sup> After UV irradiation, the charge carriers stored in the shallow trap will be released at a fast ratio and then the trapped carriers at the deeper traps slightly decrease simultaneously after a delay of 30 min. In other words, codoping  $\text{Tb}^{3+}$  ion extremely increases the number of the shallow traps but not the deeper traps, which are important for the lengthening of the persistent luminescence and thus codoping  $\text{Tb}^{3+}$  ion greatly enhances the initial LLP intensity. On

the contrary, codoping  $\text{Dy}^{3+}$  ion yields a new strong TL peak centered at high temperature (381 K). However, the temperature located far above room temperature corresponding to deep trap explains the weak LLP intensity.

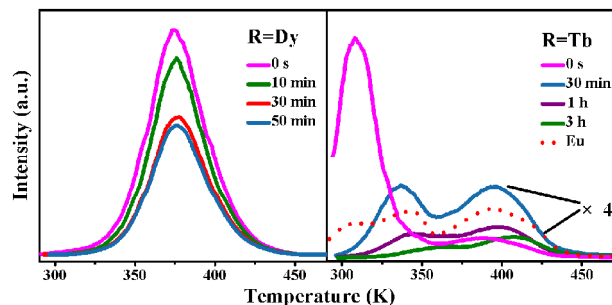


Fig. 7 The TL glow curves of  $\text{Ca}_6\text{BaP}_4\text{O}_{17}:\text{Eu}^{2+},\text{Dy}^{3+}$  and  $\text{Ca}_6\text{BaP}_4\text{O}_{17}:\text{Eu}^{2+},\text{Tb}^{3+}$  after UV irradiation for 2 min and then delaying for different time.

For the samples codoped with  $\text{Ce}^{3+}/\text{Gd}^{3+}/\text{Nd}^{3+}$  ions as shown in Fig. 8 and Fig. 9, the intensity of the TL bands decreases as the delay time increases. However, the position of the high TL intensity peak seems to move slightly to higher temperature with longer delay time, which illustrates that the trap levels continuously distribute to form a wide range of trap depth and the fading rate of the low temperature is much quicker than that of the high temperature caused by the fact that the release of the carriers from the shallow traps is much easier than the deep traps.<sup>29</sup> It is also believed that a continuous distribution of trap depth can more intuitively describe the actual situation of the inorganic phosphor defects for the reason that random variations of the nearest neighbor bond angles and bond lengths around the traps may occur.<sup>30</sup> The  $\text{Ce}^{3+}$  and  $\text{Gd}^{3+}$  ions yield appropriate traps and the  $\text{Nd}^{3+}$  ions create slightly so deep traps for efficient persistent luminescence, which explain why  $\text{Ce}^{3+}$ ,  $\text{Gd}^{3+}$ ,  $\text{Nd}^{3+}$  ions codoping have great effect on the intensity and the length of the afterglow of  $\text{Ca}_6\text{BaP}_4\text{O}_{17}:\text{Eu}^{2+}$ .

In the decay period of the phosphor codoped with  $\text{Ce}^{3+}$  ion, the TL intensity of low temperature peak decreases while high temperature peak increases simultaneously. Fig. 9 also shows that not only the position of the TL intensity peak shifts to higher temperature but also the TL intensity of high temperature peak increases with longer delay time in the phosphor codoped with  $\text{Nd}^{3+}$  ion. All the results imply that the process of retrapping by deeper traps occurs and thermally activated carriers stored in the shallower traps retrapped by deeper traps.<sup>31</sup> With assistance of the retrapping processes by the deep traps, the decay tail decreases slowly and results in longer LLP in  $\text{Ca}_6\text{BaP}_4\text{O}_{17}:\text{Eu}^{2+},\text{Ce}^{3+}$  and  $\text{Ca}_6\text{BaP}_4\text{O}_{17}:\text{Eu}^{2+},\text{Nd}^{3+}$ . Besides, due to the decrease of TL intensity of the high temperature peak, we thus deem that the carriers detrapped from the deeper traps probably by tunneling.<sup>32</sup>

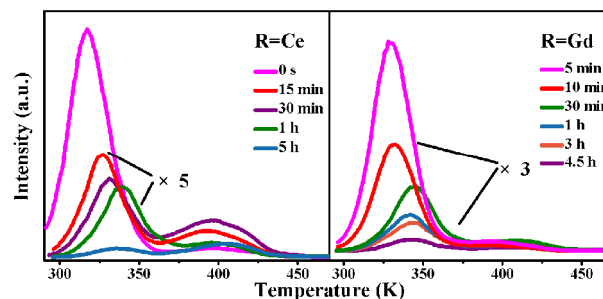


Fig. 8 The TL glow curves of  $\text{Ca}_6\text{BaP}_4\text{O}_{17}:\text{Eu}^{2+},\text{Ce}^{3+}$  and  $\text{Ca}_6\text{BaP}_4\text{O}_{17}:\text{Eu}^{2+},\text{Gd}^{3+}$  after UV irradiation for 2 min and then delaying for different time.

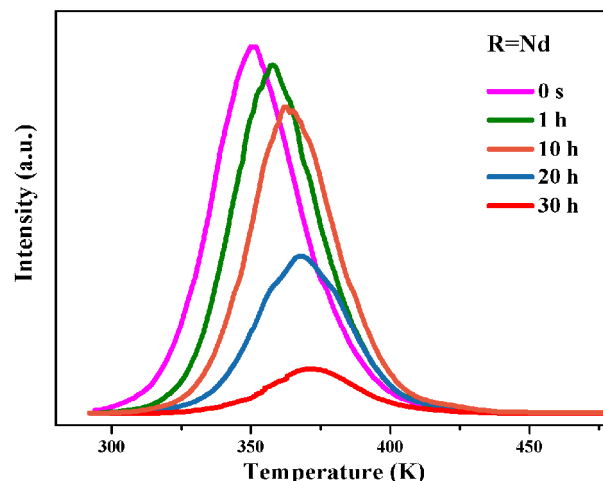


Fig. 9 The TL glow curves of  $\text{Ca}_6\text{BaP}_4\text{O}_{17}:\text{Eu}^{2+},\text{Nd}^{3+}$  after UV irradiation for 2 min and then delaying for different time.

### 3.5. The persistent luminescent mechanism of $\text{Ca}_6\text{BaP}_4\text{O}_{17}:\text{Eu}^{2+},\text{R}^{3+}$ ( $\text{R}=\text{Dy},\text{Tb},\text{Ce},\text{Gd},\text{Nd}$ ).

The mechanism of persistent luminescence is summarized in Fig. 10, which displays a schematic energy level diagram of  $\text{Eu}^{2+}$  and  $\text{R}^{3+}$  codoped  $\text{Ca}_6\text{BaP}_4\text{O}_{17}$ . Under UV irradiation, the ground-state electrons of  $\text{Eu}^{2+}$  ion are promoted to the 5d electron state. The excited electrons are trapped by shallow electron traps or deep electron traps (0.620 eV, 0.634 eV, 0.648 eV, 0.716 eV, 0.762 eV, respectively) through the conduction band. Upon thermal activation, the electrons are released from traps and then transferred to the emission centers, followed by the recombination and finally resulting in the LLP. After the exhaustion of shallow traps, the electrons located at the low-energy excited state can be directly trapped by the nearby energy-matched deep traps via tunneling, instead of going through the conduction band. In this moment, the persistent luminescence mainly originates from the tunneling effect, leading to relatively weaker LLP intensity but longer LLP duration time during the slow-decay process.

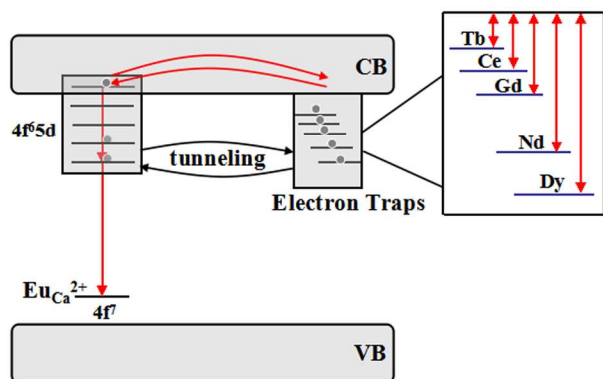
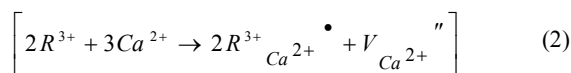


Fig. 10 Schematic energy level diagram of  $\text{Eu}^{2+}$  and  $\text{R}^{3+}$  ( $\text{R}=\text{Dy}, \text{Tb}, \text{Ce}, \text{Gd}, \text{Nd}$ ) in  $\text{Ca}_6\text{BaP}_4\text{O}_{17}$ .

In this case, the codoped trivalent  $\text{R}^{3+}$  ions chemically nonequivalently substitutes the parts of the divalent alkaline earth cation  $\text{Ca}^{2+}$  sites in the host of  $\text{Ca}_6\text{BaP}_4\text{O}_{17}:\text{Eu}^{2+}$ .<sup>11</sup> In order to make the charge balance, one possible way is that two  $\text{R}^{3+}$  ions replace three  $\text{Ca}^{2+}$  ions resulting one  $\text{V}_{\text{Ca}}$  negative defect and two  $\text{R}_{\text{Ca}}$  positive defects.<sup>33,34</sup> The defects reaction equation is shown as follows:



The other possibility is that  $\text{V}_{\text{Ca}}$  negative defects and  $\text{V}_{\text{O}}$  positive defects are generated during the synthesis process in reducing atmosphere.<sup>35-38</sup> The  $\text{R}_{\text{Ca}}$  and  $\text{V}_{\text{O}}$  positive defects are expected to act as electron traps. According to the fading of TL, we suppose that the persistent luminescence may be mainly ascribed to the new positive defects of  $\text{R}_{\text{Ca}}$  in  $\text{Ca}_6\text{BaP}_4\text{O}_{17}:\text{Eu}^{2+}$ .  $\text{R}^{3+}$ , and the intrinsic traps of  $\text{V}_{\text{Ca}}$  and  $\text{V}_{\text{O}}$  positive defects have a small effect on the afterglow performance. In the present case, the introduction of  $\text{Ce}^{3+}$ ,  $\text{Gd}^{3+}$  and  $\text{Nd}^{3+}$  ions into the host of  $\text{Ca}_6\text{BaP}_4\text{O}_{17}:\text{Eu}^{2+}$  produce a series of suitable traps, which make an important contribution to the LLP phenomenon in this kind of material. So the defects are very important for capturing and storing charge carriers (electrons and/or holes) in LLP phosphor. Nevertheless, the mechanism of LLP in  $\text{Ca}_6\text{BaP}_4\text{O}_{17}:\text{Eu}^{2+}$ .  $\text{R}^{3+}$  is still needed further research.

#### 4. Conclusions

The trap distribution of the depth and shape was estimated with the aid of LLP spectra and TL experiments with varying delay time after ceasing the UV irradiation. All  $\text{R}^{3+}$  ( $\text{R}=\text{Dy}, \text{Tb}, \text{Ce}, \text{Gd}, \text{Nd}$ ) ions did not have the same effect on the TL properties of  $\text{Ca}_6\text{BaP}_4\text{O}_{17}:\text{Eu}^{2+}$ .  $\text{Dy}^{3+}$  and  $\text{Tb}^{3+}$  ions create discrete traps and the traps are located far below or above room temperature leading to relatively poor persistent performance. While,  $\text{Ce}^{3+}$ ,  $\text{Gd}^{3+}$  and  $\text{Nd}^{3+}$  ions yield continuous traps. The TL peaks positions of the samples codoped with  $\text{Ce}^{3+}$  or  $\text{Gd}^{3+}$  ions are just above room temperature and it explains why an intense and long-lasting luminescence is observed. Although the sample codoped with  $\text{Nd}^{3+}$  ion has the longest LLP time lasting near 37.9 h, the initial brightness is only about 0.028  $\text{cd}/\text{m}^2$  due to that the traps are so deep for efficient persistent luminescence and the thermal energy at room temperature is not sufficient to induce a significant

electron to release from deep traps. Significantly, the exact knowledge of the trap distribution and the possible persistent luminescence mechanism would greatly facilitate the wider application of  $\text{Ca}_6\text{BaP}_4\text{O}_{17}:\text{Eu}^{2+}, \text{R}^{3+}$  materials and the development of new persistent luminescence materials.

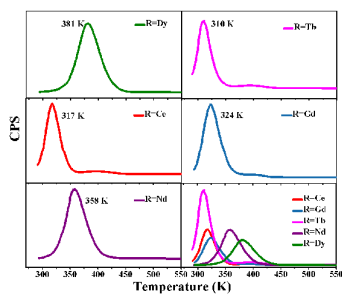
#### Acknowledgments

This work is supported by Specialized Research Fund for the Doctoral Program of Higher Education (No. 20120211130003) 35 and the National Natural Science Funds of China (Grant No. 51372105). Thanks for the support of Gansu Province Development and Reform Commission.

#### Notes and references

- Department of Materials Science, School of Physical Science and Technology, Lanzhou University, Lanzhou, 730000, PR China and Key Laboratory for Special Function Materials and Structural Design of the Ministry of Education, Lanzhou University, Lanzhou 730000, China. \*Corresponding author: Yuhua Wang
- Email address: wyh@lzu.edu.cn; tel.: +86 931 8912772; fax: +86 931 8913554.
- T. Aitasalo, J. Hölsä, H. Jungner, M. Lastusaari and J. Niittykoski, *J Phys Chem B.*, 2006, **110**, 4589-98.
- B. Wang, H. Lin, Y. Yu, D. Chen, R. Zhang, J. Xu and Y. Wang, *J. Am. Ceram. Soc.*, 2014, **97**, 2539-2545.
- C. N. Xu, T. Watanabe, M. Akiyama and X. G. Zheng, *Appl. Phys. Lett.*, 1999, **74**, 2414-2416.
- C. N. Xu, X. G. Zheng, M. Akiyama, K. Nonaka and T. Watanabe, *Appl. Phys. Lett.*, 2000, **76**, 179-181.
- M. Akiyama, C. N. Xu, Y. Liu, K. Nonaka and T. Watanabe, *J. Lumin.*, 2002, **97**, 13-18.
- T. Maldiney, A. Bessière, J. Seguin, E. Teston, S. K. Sharma, B. Viana, A. J. J. Bos, P. Dorenbos, M. Bessodes, D. Gourier, D. Scherman and C. Richard, *Nat. Mater.*, 2014, **13**, 418-426.
- K. Van den Eeckhout, P. F. Smet and D. Poelman, *Materials*, 2010, **3**, 2536-2566.
- Y. Lin, Z. Tang, Z. Zhang, X. Wang and J. Zhang, *J Mater Sci Lett.*, 2001, **20**, 1505-6.
- Y. Lin, Z. Tang, Z. Zhang and C. W. Nan, *Appl Phys Lett.*, 2002, **81**, 996-8.
- H. Yamamoto, T. Matsuzawa, *J. Lumin.*, 1997, **72**, 287-9.
- N. Komuro, M. Mikami, Y. Shimomura, E. Bithell and A. K. Cheetham, *J. Mater. Chem. C.*, 2014, **2**, 6084-6089.
- H. J. Guo, W. B. Chen, W. Zeng, G. Li, Y. H. Wang, Y. Y. Li, Y. Li and X. Ding, *J. Mater. Chem. C.*, 2015, **3**, 5844-5850.
- A. Lecointre, A. Bessière, A. J. J. Bos, P. Dorenbos, B. Viana and S. Jacquart, *J. Phys. Chem. C*, 2011, **115**, 4217-4227.
- S. W. S. McKeever and R. Chen, *Radiat Meas.*, 1997, **27**, 625-628.
- T. Maldiney, A. Lecointre, B. Viana, A. Bessière, M. Bessodes, D. Gourier, C. Richard and D. Scheman, *J. Am. Ceram. Soc.*, 2011, **133**, 11810-11815.
- B. Zhang, X. Xu, Q. Li, Y. Wu, J. Qiu and X. Yu, *Journal of Solid State Chemistry*, 2014, **217**, 136-141.
- Z. Pan, Y. Y. Lu and F. Liu, *Nat. Mater.*, 2012, **11**, 58-63.
- J. Trojan-Piegza, J. Niittykoski, J. Hölsä and E. Zych, *Chem. Mater.*, 2008, **20**, 2252-2261.
- P. Avouris, *J. Chem. Phys.*, 1981, **74**, 4347-4355.

20. P. Dorenbos, A. H. Krumpel, E. van der Kolk, P. Boutinaud, M. Bettinelli and E. Cavalli, *Opt. Mater.*, 2010, **32**, 1681-1685.
21. P. Dorenbos and A. J. J. Bos, *Radiat. Measure*, 2008, **43**, 39-145.
22. R. Chen, *Journal of Materials Science*, 1976, **11**, 1521-1541.
- 5 23. X. Sun, J. Zhang, X. Zhang, Y. Luo and X. J. Wang, *J. Phys. D:Appl. Phys.*, 2008, **41**, 195414.
24. Y. Liu, B. Lei and C. Shi, *Chem. Mater.*, 2004, **17**, 2108-2113.
25. C. S. Shalgaonkar, A. V. Narlikar, *J. Mater. Sci.*, 1972, **7**, 1465-1471.
26. J. C. Zhang, M. H. Yu, Q. S. Qin, H. L. Zhou, M. J. Zhou, X. H. Xu  
10 and Y. H. Wang, *J. Appl. Phys.*, 2010, **108**, 123518.
27. C. Q. Wu, J. C. Zhang, P. F. Feng, Y. M. Duan, Z. Y. Zhang and Y. H. Wang, *Journal of Luminescence*, 2014, **147**, 229234.
28. Y. L. Jia, H. F. Li, R. Zhao, W. Z. Sun, Q. Su, R. Pang and C. Y. Li, *Optical Materials*, 2014, **36**, 1781-1786.
- 15 29. Y. H. Jin, Y. H. Hu, L. Chen, Y. R. Fu, Z. F. Mu, T. Wang and J. Lin, *Journal of Alloys and Compounds*, 2014, **616**, 159-165.
30. K. Van den Eeckhout, A. J. J. Bos, D. Poelman and P. F. Smet, *Physical Review B*, 2013, **87**, 045126.
31. X. Yu, T. Wang, X. H. Xu, D. C. Zhou and J. B. Qiu, *ECS Solid State Lett.*, 2014, **3**, R4-R6.
- 20 32. W. B. Chen, Y. H. Wang, W. Zeng, S. C. Han and G. Li, *Optical Materials*, 2014, **36**, 1850-1854.
33. J. Wang, S. B. Wang and Q. Su, *J. Mater. Chem.*, 2004, **14**, 2569.
34. B. F. Lei, Y. L. Liu, J. Liu, Z. R. Ye and C. S. Shi, *J. Solid State Chem.*, 2004, **177**, 1333.
- 25 35. J. Qiu and K. Hirao, *Solid State Commun.*, 1998, **106**, 795-798.
36. F. Clabau, X. Rocquefelte, S. Jobic, P. Deniard, M. H. Whangbo, A. Garcia and T. Le Mercier, *Chem.Mater.*, 2005, **17**, 3904-3912.
37. J. Trojan-Piegza, J. Niittykoski, J. Hölsä and E. Zych, *Chem.Mater.*,  
30 2008, **20**, 2252-2261.
38. J. Wang, S. Wang and Q. Su, *J. Solid State Chem.*, 2004, **177**,895-900.



Controlling and revealing trap distributions of  $\text{Ca}_6\text{BaP}_4\text{O}_{17}:\text{Eu}^{2+},\text{R}^{3+}$  ( $\text{R}=\text{Dy}, \text{Tb}, \text{Ce}, \text{Gd}, \text{Nd}$ ) by codoping different trivalent lanthanides.